**Supporting Information**

# Transport Properties of Ba(Zr,Ce,Y,Yb)$O_{3-\delta}$ Proton Conductor: the Real Role of Co-Substitution of Y and Yb

Hui Guo [1,+], Yifeng Li [1,+], Lulu Jiang [1], Yenan Sha [1], Shihang Guo [1], Donglin Han [1,2,3,4*]

[1] College of Energy, Soochow University, No 1 Shizi Street, Gusu District, Suzhou 215006, China

[2] Provincial Key Laboratory for Advanced Carbon Materials and Wearable Energy Technologies, Soochow University, No 1 Shizi Street, Gusu District, Suzhou 215006, China

[3] Jiangsu Key Laboratory of Advanced Negative Carbon Technologies, Soochow University, Suzhou 215123, China

[4] Light Industry Institute of Electrochemical Power Sources, Shahu Science & Technology Innovation Park, Suzhou 215638, China

[+] These authors contributed equally.

* Corresponding author: Donglin Han (dlhan@suda.edu.cn)

## 1. XRD Patterns

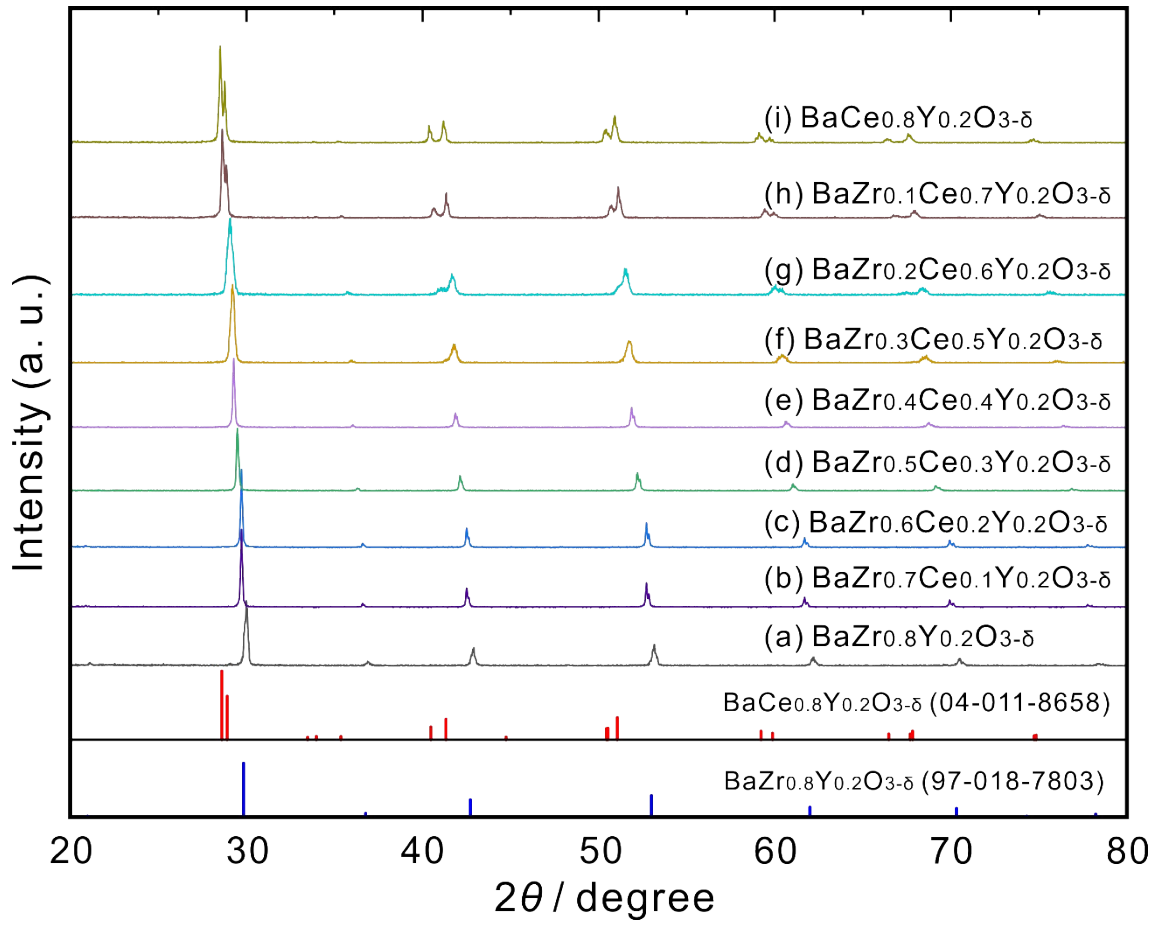


**Figure S1** Powder XRD patterns of (a) $BaZr_{0.8}Y_{0.2}O_{3-\delta}$, (b) $BaZr_{0.7}Ce_{0.1}Y_{0.2}O_{3-\delta}$, (c) $BaZr_{0.6}Ce_{0.2}Y_{0.2}O_{3-\delta}$, (d) $BaZr_{0.5}Ce_{0.3}Y_{0.2}O_{3-\delta}$, (e) $BaZr_{0.4}Ce_{0.4}Y_{0.2}O_{3-\delta}$, (f) $BaZr_{0.3}Ce_{0.5}Y_{0.2}O_{3-\delta}$, (g) $BaZr_{0.2}Ce_{0.6}Y_{0.2}O_{3-\delta}$, (h) $BaZr_{0.1}Ce_{0.7}Y_{0.2}O_{3-\delta}$ and (i) $BaCe_{0.8}Y_{0.2}O_{3-\delta}$ after sintering.

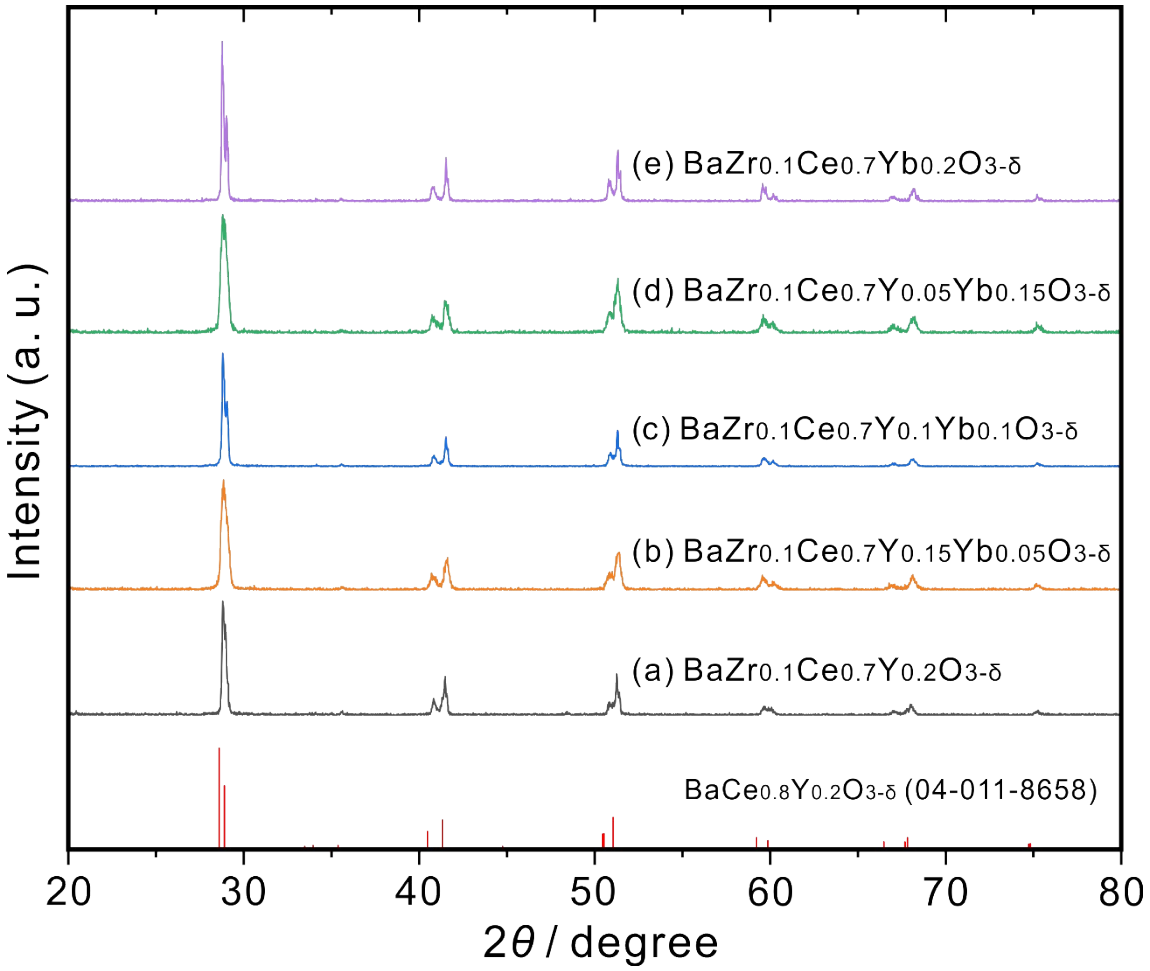


**Figure S2** Powder XRD patterns of (a) $BaZr_{0.1}Ce_{0.7}Y_{0.2}O_{3-\delta}$, (b) $BaZr_{0.1}Ce_{0.7}Y_{0.15}Yb_{0.05}O_{3-\delta}$, (c) $BaZr_{0.1}Ce_{0.7}Y_{0.1}Yb_{0.1}O_{3-\delta}$, (d) $BaZr_{0.1}Ce_{0.7}Y_{0.05}Yb_{0.15}O_{3-\delta}$ and (e) $BaZr_{0.1}Ce_{0.7}Yb_{0.2}O_{3-\delta}$ after sintering.

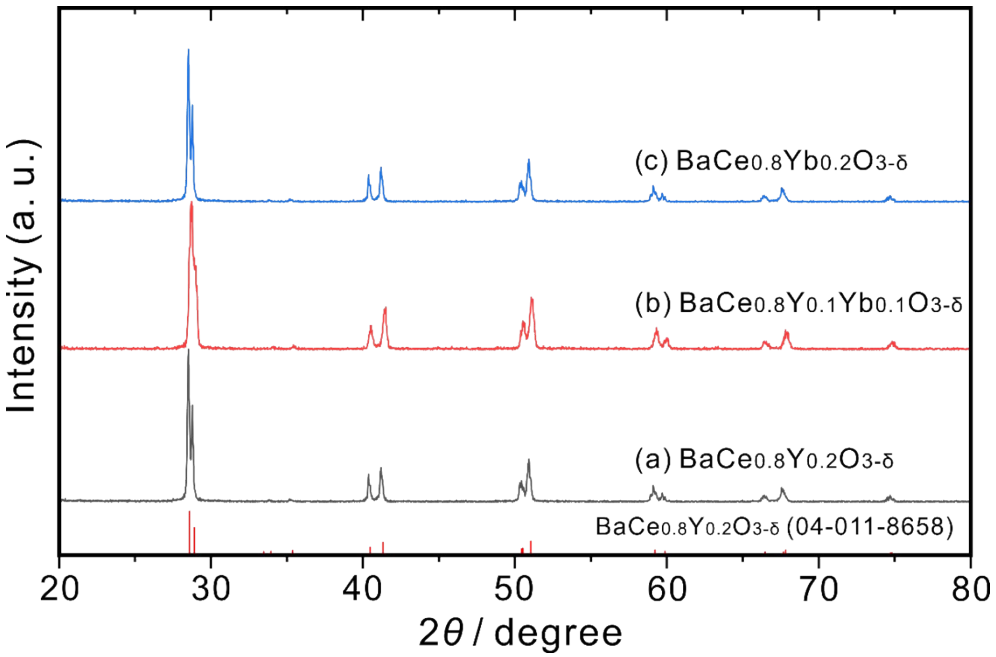


**Figure S3** Powder XRD patterns of (a) $BaCe_{0.8}Y_{0.2}O_{3-\delta}$, (b) $BaCe_{0.8}Y_{0.1}Yb_{0.1}O_{3-\delta}$ and (c) $BaCe_{0.8}Yb_{0.2}O_{3-\delta}$ after sintering.

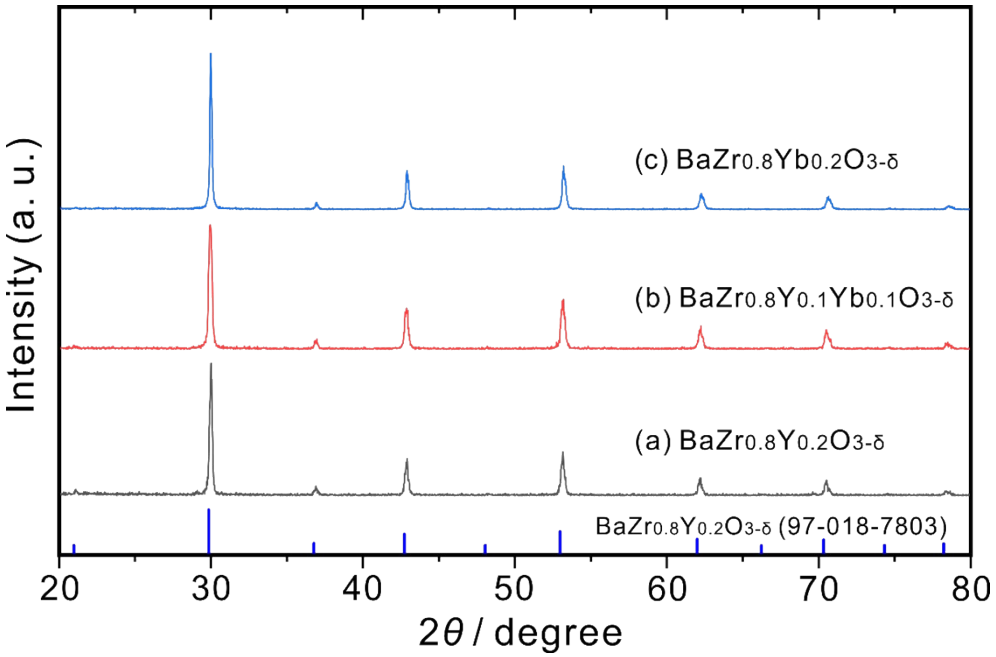


**Figure S4** Powder XRD patterns of (a) $BaZr_{0.8}Y_{0.2}O_{3-\delta}$, (b) $BaZr_{0.8}Y_{0.1}Yb_{0.1}O_{3-\delta}$ and (c) $BaZr_{0.8}Yb_{0.2}O_{3-\delta}$ after sintering.

## 2. SEM Images

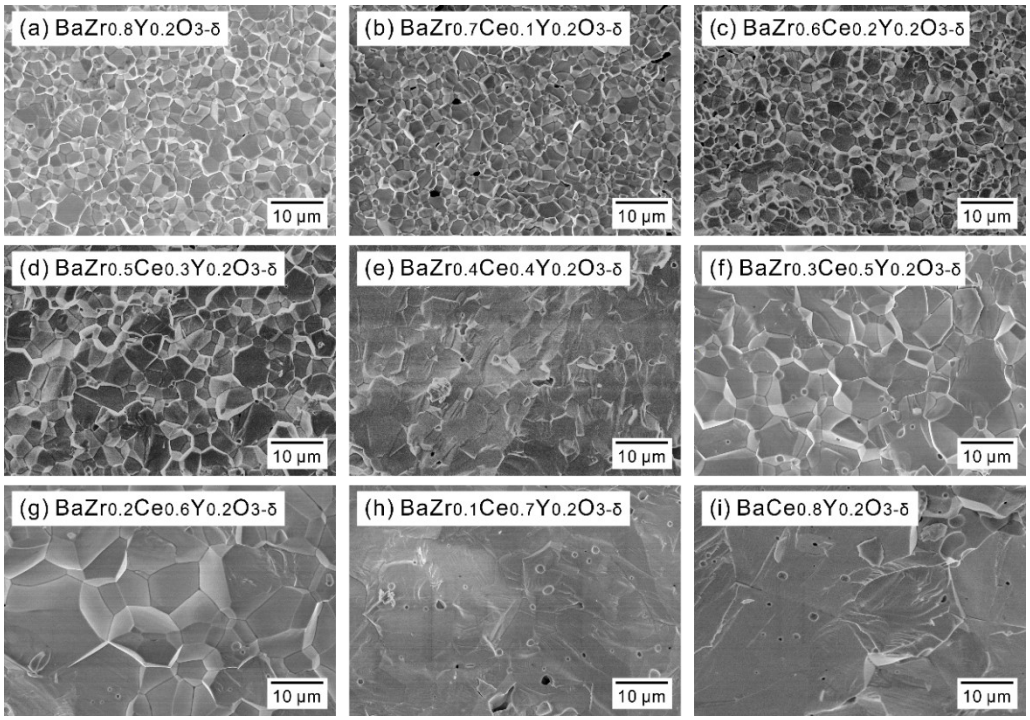


**Figure S5** SEM images of fractured cross-section of as-sintered (a) $BaZr_{0.8}Y_{0.2}O_{3-\delta}$, (b) $BaZr_{0.7}Ce_{0.1}Y_{0.2}O_{3-\delta}$, (c) $BaZr_{0.6}Ce_{0.2}Y_{0.2}O_{3-\delta}$, (d) $BaZr_{0.5}Ce_{0.3}Y_{0.2}O_{3-\delta}$, (e) $BaZr_{0.4}Ce_{0.4}Y_{0.2}O_{3-\delta}$, (f) $BaZr_{0.3}Ce_{0.5}Y_{0.2}O_{3-\delta}$, (g) $BaZr_{0.2}Ce_{0.6}Y_{0.2}O_{3-\delta}$, (h) $BaZr_{0.1}Ce_{0.7}Y_{0.2}O_{3-\delta}$ and (i) $BaCe_{0.8}Y_{0.2}O_{3-\delta}$.

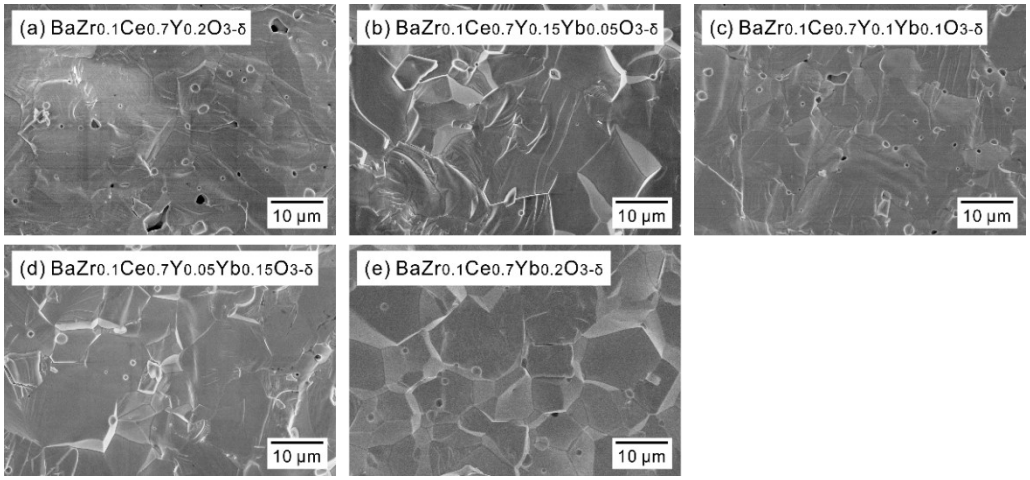


**Figure S6** SEM images of fractured cross-section of as-sintered (a) $BaZr_{0.1}Ce_{0.7}Y_{0.2}O_{3-\delta}$, (b) $BaZr_{0.1}Ce_{0.7}Y_{0.15}Yb_{0.05}O_{3-\delta}$, (c) $BaZr_{0.1}Ce_{0.7}Y_{0.1}Yb_{0.1}O_{3-\delta}$, (d) $BaZr_{0.1}Ce_{0.7}Y_{0.05}Yb_{0.15}O_{3-\delta}$ and (e) $BaZr_{0.1}Ce_{0.7}Yb_{0.2}O_{3-\delta}$.

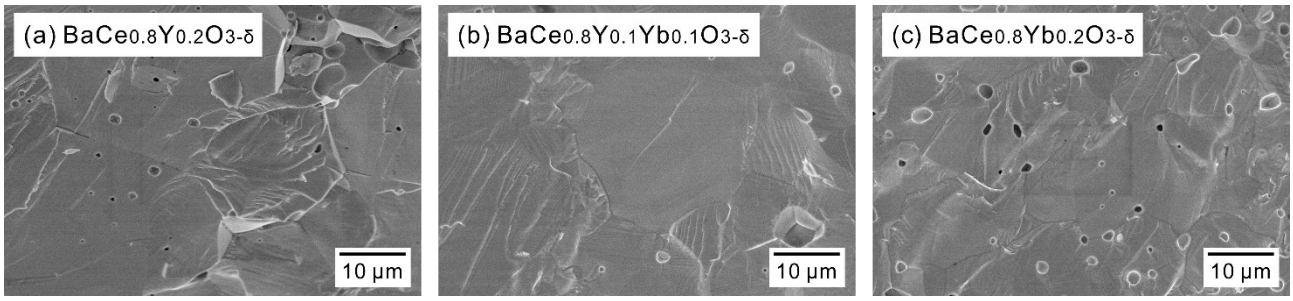


**Figure S7** SEM images of fractured cross-section of as-sintered (a) $BaCe_{0.8}Y_{0.2}O_{3-\delta}$, (b) $BaCe_{0.8}Y_{0.1}Yb_{0.1}O_{3-\delta}$ and (c) $BaCe_{0.8}Yb_{0.2}O_{3-\delta}$.

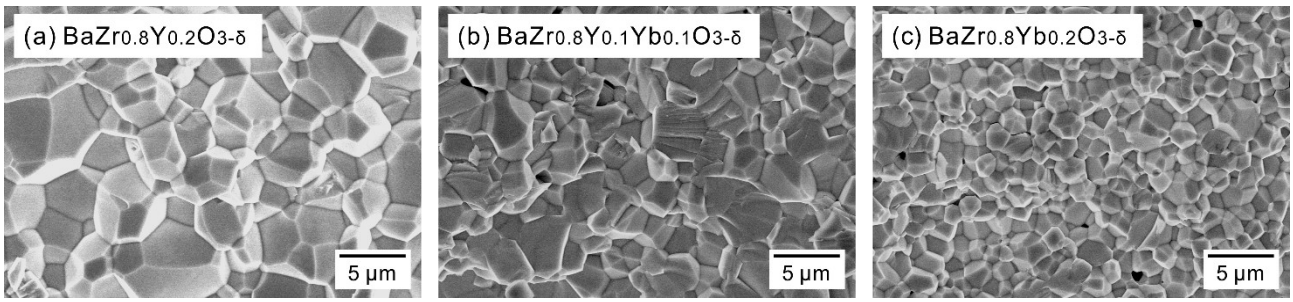


**Figure S8** SEM images of fractured cross-section of as-sintered (a) $BaZr_{0.8}Y_{0.2}O_{3-\delta}$, (b) $BaZr_{0.8}Y_{0.1}Yb_{0.1}O_{3-\delta}$ and (c) $BaZr_{0.8}Yb_{0.2}O_{3-\delta}$.

## 3. EMF Measurements

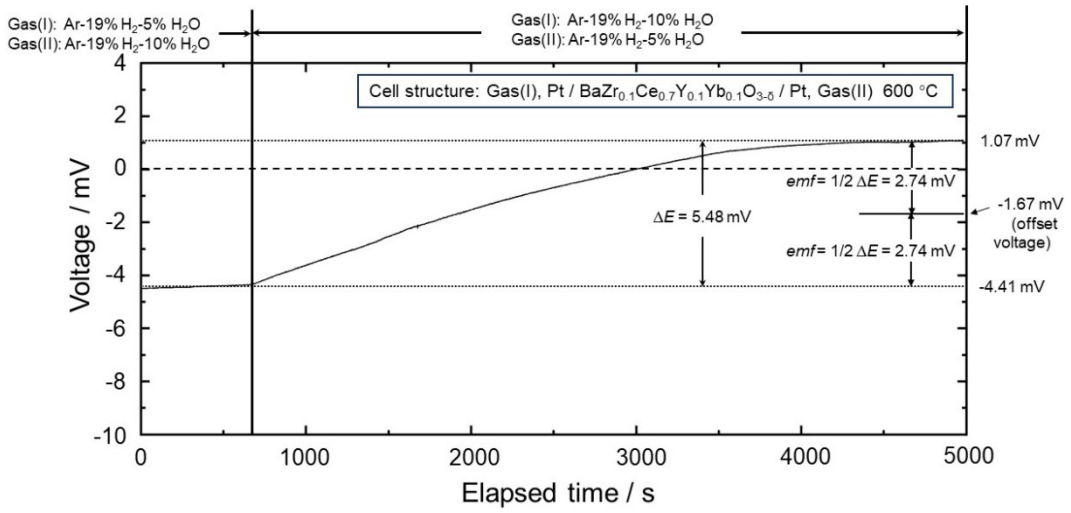


**Figure S9** Change of voltage of $BaZr_{0.1}Ce_{0.7}Y_{0.1}Yb_{0.1}O_{3-\delta}$ with the elapsed time during switching the gas fed to the two electrodes at 600 °C.